Dynamical entanglement formation and dissipation effects in two double quantum dots

2006 J. Phys.: Condens. Matter 18 9771

(http://iopscience.iop.org/0953-8984/18/43/001)

INSTITUTE OF PHYSICS PUBLISHING JOURNAL OF PHYSICS: CONDENSED MATTER

J. Phys.: Condens. Matter **18** (2006) 9771–9782 doi:10.1088/0953-8984/18/43/001

Dynamical entanglement formation and dissipation effects in two double quantum dots

L D Contreras-Pulido[1] **and F Rojas**[2]

[1] Centro de Investigación Científica y de Educación Superior de Ensenada, Apartado Postal 2732, Ensenada, BC 22860, Mexico
[2] Departamento de Física Teórica, Centro de Ciencias de la Materia Condensada, Universidad Nacional Autónoma de México, Ensenada, Baja California 22800, Mexico

E-mail: debora@ccmc.unam.mx and frojas@ccmc.unam.mx

Received 7 April 2006, in final form 21 September 2006
Published 13 October 2006
Online at stacks.iop.org/JPhysCM/18/9771

Abstract

We study the static and dynamic formation of entanglement in charge states of a two double quantum dot array with two mobile electrons under the effect of an external driving field. We include dissipation via contact with a phonon bath. By using the density matrix formalism and an open quantum system approach, we describe the dynamical behaviour of the charge distribution (polarization), concurrence (measure of the degree of entanglement) and Bell state probabilities (two qubit states with maximum entanglement) of such a system, including the role of dot asymmetry and temperature effects. Our results show that it is possible to obtain entangled states as well as a most probable Bell state, which can be controlled by the driving field. We also evaluate how the entanglement formation based on charge states deteriorates as the temperature or asymmetry increases.

(Some figures in this article are in colour only in the electronic version)

1. Introduction

Entanglement is a quantum mechanical property with no classical counterpart; it corresponds to the joint state of two or more quantum systems and describes correlations between them that are much stronger than any classical correlation [1]. It is an important source for quantum computing and an essential element for quantum communication schemes (such as quantum dense code, quantum teleportation and quantum cryptography [1, 2]). Therefore, there is currently great interest in finding systems to implement and control both entangled states (defined as non-separable superpositions of its component states [1, 2]) and the basic unit for quantum computers named qubit.

There have been different proposals to produce entangled states, such as atomic systems [1, 3], semiconductor quantum dots [4] and other schemes based on spins and

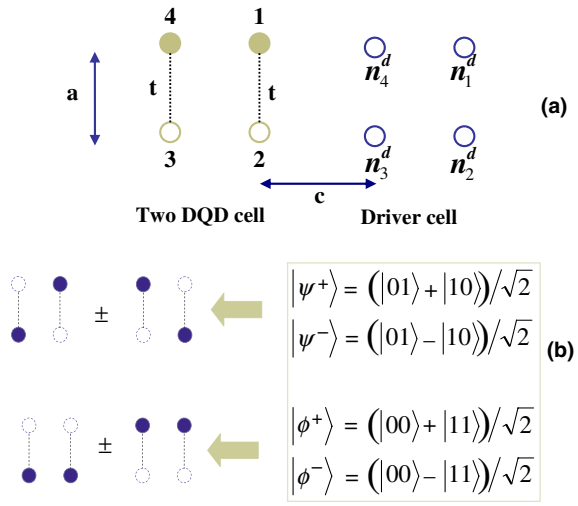

$$|\psi^{+}\rangle = \left(|01\rangle + |10\rangle\right)/\sqrt{2}$$
$$|\psi^{-}\rangle = \left(|01\rangle - |10\rangle\right)/\sqrt{2}$$
$$|\phi^{+}\rangle = \left(|00\rangle + |11\rangle\right)/\sqrt{2}$$
$$|\phi^{-}\rangle = \left(|00\rangle - |11\rangle\right)/\sqrt{2}$$

Figure 1. Diagrams for: (a) the two double quantum dot cell (tunnelling allowed vertically only) in the presence of driver cell with charge density n_i^d in each QD. It is possible to encode two charge qubits with the electron located in each double dot. (b) Definition of the Bell states $|\Psi^{\pm}\rangle$, $|\phi^{\pm}\rangle$ on the two qubit basis and expressed in terms of linear combinations of charge distribution inside the square cell.

cavities [1, 5, 6]. Among the systems proposed for qubit implementation, those based on the charge degree of freedom (called charge qubits [7, 8]) and specifically constructed with solid state systems such as double quantum dots (DQDs) [4, 7, 9, 10] are important candidates because of scalability [6], making a natural connection with current microelectronics and offering a good control of a single charge qubit [11]. In addition, arrays of interacting quantum dots (QDs) have been proposed as elements for encoding, processing and transmitting logical information and even for the physical realization of a quantum computer [12] based on quantum and classical effects [13].

Here, we investigate entanglement formation in two charge qubits formed by a two double quantum dot array (which can represent a basis for a 'quantum register'), including the effect of the environment and possible dot imperfections.

The basic unit of this system, or cell, has four quantum dots at the corners of a square with two extra electrons. When we include the Coulomb interaction and tunnelling, the ground state has two equally probable states with the electrons aligned on opposite corners. These 'polarization' states (+1 and −1, as defined below (equation (7)) and in [13]) are degenerate and have been used to encode two bits of classical information [12, 13] and as a basis for the charge qubits [7]. The degeneracy is broken by the effect of an externally controlled time-dependent field, which can be thought of as a driver cell. This field produces the desired electric potential on the array, allowing the control of charge in the states of the QD array, and possibly of entanglement. Our scheme is based on recent experimental realization of a charge qubit manipulated with time-dependent pulsed gate voltages or microwaves [10, 11].

We propose a cell where the electrons can tunnel only vertically between neighbour dots (figure 1(a)). Thus, in effect, we have two DQDs coupled by Coulomb interactions representing two charge qubits. The main purpose of the present paper is to explore the formation of entanglement based on the charge distribution inside the two DQD cell, through the control of the driver cell polarization.

Because solid state devices are not free from fabrication imperfections, we also take into account asymmetry effects in the cell behaviour when the energy level of one of the QDs is changed by a certain amount. On the other hand, in ideal situations, quantum coherence must be maintained during quantum computing processes; however the interaction of the qubits with the environment inevitably disturbs the desired quantum evolution of that process, and the effect of surrounding phonons is the major cause of decoherence in such qubit implementation [6, 16]. Therefore, we also include the coupling of the cell electrons to a bath of phonons in thermal equilibrium.

Even though there are different ways to evaluate if a quantum system is entangled, many authors [4, 17–19] have recently used Wootters' concurrence for two qubits, which is applied for pure and mixed ensembles, and its calculation is based on the density matrix of the systems [20]. We use concurrence to characterize the degree of entanglement in our two DQD system, in both coherent and decoherent or dissipative dynamics.

Besides charge distribution and entanglement, we evaluate the formation of Bell states (states of two qubits with the maximum entanglement [1, 2, 20], figure 1(b)), due to their importance in quantum information and communication applications.

For coherent dynamics, we study the system by solving the time evolution of the density matrix for the two double dot cell taking into account a linear time-dependent driver cell polarization, intracell Coulomb interactions and imperfection effects. Using a Markovian master equation approach for the reduced density matrix of the system, we consider dissipation effects via electron–phonon interactions in each dot. For both dynamical analyses, our results show that entangled states and a specific most probable Bell state can be obtained in a controlled electrical scheme.

2. Model

The two DQD cell in the presence of a driver cell is described by a Hubbard-type Hamiltonian which includes intracell and intercell Coulomb repulsion as well as tunnelling inside the cell [13, 21]:

$$H_S = \sum_i \epsilon_i \hat{n}_i + t \sum_{\langle ij \rangle} (\hat{c}_i^\dagger \hat{c}_j + \hat{c}_j^\dagger \hat{c}_i) + \sum_{i>j} V_{ij} \hat{n}_i \hat{n}_j + \sum_{i,j} W_{ij} \hat{n}_i^d(t) \hat{n}_j \qquad (1)$$

where $\hat{c}_i^\dagger$ ($\hat{c}_i$) is the creation (annihilation) operator of electrons and $\hat{n}_i$ is the number operator. ϵ_j is the on-site energy at the ith quantum dot in the DQD cell, where we can add asymmetry effects by changing the energy level in a given QD by δ (a measure of the imperfections due to different dot size or a change in the local environment). The electron tunnelling between nearest-neighbour dots inside the cell is t, and it is allowed only vertically in our model. $V_{ij} = V/d_{ij}$ is the electrostatic interaction between electrons in dots i and j in the two DQD cell, separated a distance d_{ij}, and W_{ij} is that between site j in the two DQD cell and site i in the driver cell (which has a general time-dependent charge density $\hat{n}_i^d(t)$). As we have mentioned, the driver cell is a controllable external potential applied on the charge qubits array produced by means of manipulation of stationary or dynamic gate voltages applied in each QD of the array. This is a coherent external electric energy which directly renormalizes on-site energy on each dot. We base our driver model on recent experimental realizations of a single charge qubit manipulated with time-dependent gate voltages [10, 11] (where coherence in the array is demonstrated for up to 200 ns); on experimental settings of similar cell systems that use gate voltages to produce only charge manipulation [14, 15] and also on theoretical studies that consider coherent drivers [16].

Notice that we assume spinless electrons and double occupancy is forbidden. Following the notation of Lent *et al* [13] the distance between quantum dots is a, while the separation between target and driver cells is c as it is shown in figure 1.

We consider the dissipative model introduced in [16, 22] which consists of a reservoir (bath) of phonons represented by a set of quantum harmonic oscillators of frequency ω_k, given by $H_{\mathrm{R}} = \sum_k \hbar\omega_k \hat{b}_k^\dagger \hat{b}_k$, where $\hat{b}_k^\dagger$ ($\hat{b}_k$) is the creation (annihilation) phonon operator. It also includes the electron–phonon interaction in the form

$$V_{\mathrm{SR}} = \sum_k \sum_{\langle i,j\rangle} \alpha_{kij} \hat{c}_i^\dagger \hat{c}_j (\hat{b}_k^\dagger + \hat{b}_k) \tag{2}$$

where we consider the coupling parameter $\alpha_{kij} = D g_k(\omega_k)$ with D the coupling strength constant and $g_k(\omega_k) \propto \omega_k^{1/2}$ for the deformation potential model [16, 22]. Thus, for the model with dissipation the *total Hamiltonian* is given by $H = H_{\mathrm{S}} + H_{\mathrm{R}} + V_{\mathrm{SR}}$.

We assume the quantum dots to be as those defined in [16, 21] for which the intra-dot Coulomb repulsion is $V \approx 1$ meV, and this quantity is taken as the unit of energy in this paper. For our particular model, the basis is given by the four charge distribution states in the two DQD cell: $|11\rangle = |1001\rangle$, $|10\rangle = |0101\rangle$, $|01\rangle = |1010\rangle$ and $|00\rangle = |0110\rangle$, where $|n_1 n_2 n_3 n_4\rangle$ represents one electron present ($n_i = 1$) or absent ($n_i = 0$) in the ith QD (see figure 1). The states $|10\rangle$ and $|01\rangle$ correspond to charge distributed along the diagonals in the square cell, and because of electrostatic interaction they have minimum energy and can be selected by choosing a driver cell with an equivalent charge distribution. On the other hand, states $|11\rangle$ and $|00\rangle$ are configurations with electrons along the square sides and correspond to excited states. In that way, the four Bell states in the computational basis [1, 20] can be straightforwardly related to our basis states as shown in figure 1(b), where it can be noticed that they are associated with linear combinations of charge distribution states, both along the diagonals ($|\Psi^\pm\rangle = (|01\rangle \pm |10\rangle)/\sqrt{2}$) and along the sides of the DQD cell ($|\phi^\pm\rangle = (|00\rangle \pm |11\rangle)/\sqrt{2}$).

For the stationary case we solve the eigenvalue problem $H_{\mathrm{S}}\phi_n = E_n\phi_n$ and study the ground state properties. In this case, we assume a fixed driver charge configuration on sites 1 and 3 ($n_1^d = n_3^d = 1$ and $n_2^d = n_4^d = 0$) corresponding to polarization $P_{\mathrm{driver}} = +1$ (see equation (7) below). For dynamical studies we consider a driver polarization that changes linearly with time in two different switching schemes: in the first, it goes from $P_{\mathrm{driver}} = +1$ (charge on sites 1 and 3) to $P_{\mathrm{driver}} = -1$ (charge on sites 2 and 4) in a time τ, so that $P_{\mathrm{driver}}(t) = 1 - 2t/\tau$; and in the second, from $P_{\mathrm{driver}} = +1$ to 0 in a switching time $\tau/2$. This corresponds to charge densities in the driver cell of $n_1^d(t) = n_3^d(t) = 1 - t/\tau$ and $n_2^d(t) = n_4^d(t) = t/\tau$. In general, for coherent dynamics, the equation of motion for the density matrix of the system (Liouville–von Neumann equation) is solved, while for dissipation (only for the second driver polarization switching scheme) we solve the time evolution for the *reduced density matrix* (RDM) elements defined through the Markov approximation for open quantum systems. In the Schrödinger picture it is given by [16, 23]

$$\dot{\rho}_{\mathrm{S}}(t)_{ss'} = -\mathrm{i}\omega_{ss'}\rho_{\mathrm{S}}(t)_{ss'} + \sum_{mn} \tilde{\mathbf{R}}_{ss'mn}\rho_{\mathrm{S}}(t)_{mn}. \tag{3}$$

The first term on the right-hand side represents reversible (coherent) effects and depends on transition frequencies of the system $\omega_{ss'} = (E_{\mathrm{S}} - E_{\mathrm{S}'})/\hbar$ (E_m are the cell eigenenergies), and the second term describes relaxation processes (irreversible dynamics) where $\tilde{\mathbf{R}}_{ss'mn}$ is called the *relaxation tensor* [23], given explicitly as

$$\tilde{\mathbf{R}}_{ss'mn} = \begin{cases} \delta_{nm}(1-\delta_{ms})\tilde{W}_{sm} - \delta_{ms}\delta_{ns}\sum_{k\neq s}\tilde{W}_{ks} & (s = s') \\ -\gamma_{ss'}\delta_{ms}\delta_{ns'} & (s \neq s'). \end{cases} \tag{4}$$

Here, $\tilde{W}_{nm}$ are the transition rates from state $|m\rangle$ to $|n\rangle$, which can be expressed in terms of bath and DQD cell properties as

$$\tilde{W}_{mn} = \frac{2\pi}{\hbar^2} D^2 |g(\omega_{mn})|^2 \mathcal{D}(\omega_{mn}) \{ |S_{mn}|^2 \bar{n}(\omega_{mn}) + |S_{mn}|^2 [1 + \bar{n}(\omega_{mn})] \} \tag{5}$$

where $\bar{n}(\omega)$ is the mean phonon number with frequency ω (Bose–Einstein distribution), $\mathcal{D}(\omega_{mn})$ is the density of boson states ($\sim\omega^2$ in the Debye model) [16, 22] and S_{mk} are the matrix elements of the electronic part of the cell interacting with the phonon reservoir, equation (2), which can be interpreted as phonon-assisted tunnelling events. The charge states involved in such transitions are given in terms of projectors as $S = |01\rangle\langle 11| + |10\rangle\langle 11| + |01\rangle\langle 00| + |10\rangle\langle 00|$.

$\gamma_{ss'}$ in equation (4) is called the non-adiabatic parameter whose real part contributes to the time decay of the off-diagonal density matrix elements, and is directly responsible for the loss of coherence. This parameter can be written in terms of the transition rates by Re $\gamma_{ss'} = (\sum_{k\neq s} \tilde{W}_{ks} + \sum_{k\neq s} \tilde{W}_{ks'})/2$ [16]. Its imaginary part corresponds to an intrinsic relaxation rate for each transition which we assume negligible.

From equation (5), one can notice that transition rates satisfy the detailed balanced condition

$$\frac{\tilde{W}_{nm}}{\tilde{W}_{mn}} = \exp\left(-\frac{\hbar\omega_{nm}}{k_B T}\right). \tag{6}$$

The numerical solution of both stationary and dynamical equations are used to evaluate the two DQD cell properties. The cell *polarization* is calculated as [21]

$$P = \frac{\zeta_1 + \zeta_3 - (\zeta_2 + \zeta_4)}{\sum_i \zeta_i}, \tag{7}$$

where ζ_i is the charge density at QD i and is determined from the density matrix as the expectation value of the number operator at each site, $\zeta_i = \mathrm{tr}(\rho_S \hat{n}_i)$. Notice that states of charge distribution along the diagonals $|01\rangle$ and $|10\rangle$ correspond to polarization $P = 1$ and -1 respectively.

On the other hand, Wootters's expression for concurrence [20] for a pure state of two qubits is

$$C = |\langle\psi|\tilde{\psi}\rangle| \tag{8}$$

with $|\tilde{\psi}\rangle = (\sigma_y \otimes \sigma_y)|\psi^*\rangle$, where $|\psi^*\rangle$ is the complex conjugate of $|\psi\rangle$ and σ_y is the Pauli matrix. For a general state (pure or mixtures), the concurrence for two qubits is also calculated in terms of the density matrix ρ_S as

$$C = \max\{0, \lambda_1 - \lambda_2 - \lambda_3 - \lambda_4\} \tag{9}$$

where the λs are the square roots of the eigenvalues, in decreasing order, of the non-Hermitian matrix $\rho_S\tilde{\rho}_S = \rho_S(\sigma_y \otimes \sigma_y)\rho_S^*(\sigma_y \otimes \sigma_y)$, where ρ_S^* denotes the complex conjugation of ρ_S. Concurrence values go from 0 (no correlation between states) to 1 (maximum degree of entanglement); Bell states have $C = 1$ [20] and each cell state ($|11\rangle$, $|10\rangle$, $|01\rangle$ and $|00\rangle$) has null concurrence, $C = 0$.

3. Results and discussion

For the stationary study, we consider a constant driver polarization $P_{\mathrm{driver}} = +1$, and calculate the ground state properties as a function of tunnelling coupling, t/V, as shown in figure 2. From the energy spectrum (figure 2(a)) we can see that the presence of the driver cell removes the

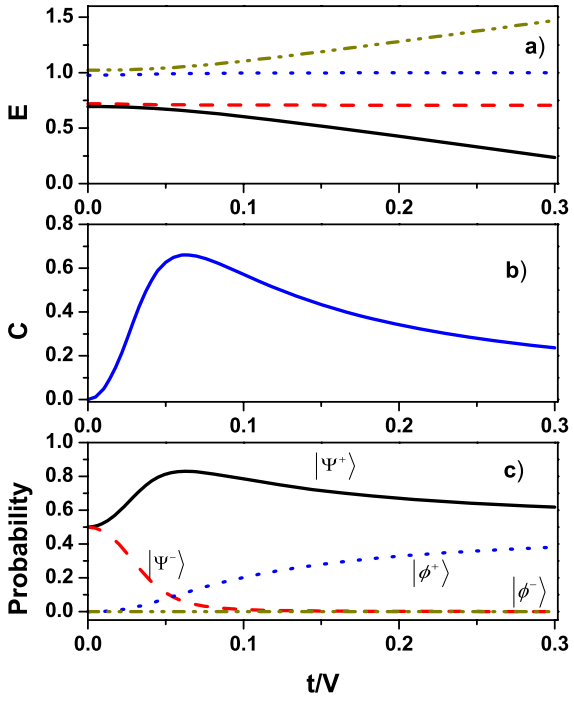

Figure 2. Ground state properties for the two DQD cell, as a function of tunnelling: (a) energy level structure, (b) concurrence and (c) stationary Bell state probabilities.

degeneracy even for $t/V = 0$, and as tunnelling increases, it produces additional level splitting. The ground state corresponds to a cell polarization $P_{\text{cell}} \cong +1$ (not shown) induced by the electrostatic driver effect, but increasing tunnelling reduces that value in agreement with results presented in [16]. On the other hand, entanglement measured through concurrence (figure 2(b)) as a function of tunnelling goes from zero (no correlation between cell states) to a maximum value (around 0.66) for a tunnelling amplitude $t_c/V = 0.063$ and then decreases, approaching zero for large values of tunnelling. This concurrence has contributions from different Bell states, $|\Psi^+\rangle$ being the one with the largest probability (which corresponds to a symmetric contribution of states with electrons along diagonals). The concurrence behaviour can be better understood by studying the model in the Bell states basis.

For this ground state, which is a pure state, concurrence can be calculated from equation (8) in terms of Bell state probabilities as $C = |P_{\Psi^+} - P_{\Psi^-} - P_{\phi^+} + P_{\phi^-}|$ (where P_i is the probability for Bell state i). From figure 2(c) one can observe that, for small tunnelling, $t/V \sim 0$, the cell is mainly formed by the combination $|01\rangle \sim (|\Psi^+\rangle + |\Psi^-\rangle)$, which is not entangled and has zero concurrence [20]. Next, there is a tunnelling regime $0 < t/V < t_c/V$ which starts to promote charge delocalization yielding a combination mainly formed by $|01\rangle$ and $|10\rangle$ states ($|\Psi^+\rangle$ and $|\Psi^-\rangle$) and a small contribution of the $|\phi^+\rangle$ state. As the $|01\rangle$ state is preferred because of the driver effect, the probability of $|\Psi^+\rangle$ increases to a larger value than that of $|\phi^+\rangle$ and also a decrease in the probability of $|\Psi^-\rangle$ is observed; thus concurrence tends to increase its value as is pointed out in the previous expression. For $t/V > t_c/V$, the two DQD cell enters in a new regime where delocalization induced by tunnelling is stronger and promotes equal population in each QD, producing a superposition of all cell states $\sim (|\Psi^+\rangle + |\phi^+\rangle)$, with a corresponding increasing of $|\phi^+\rangle$ probability that presents an adverse contribution for

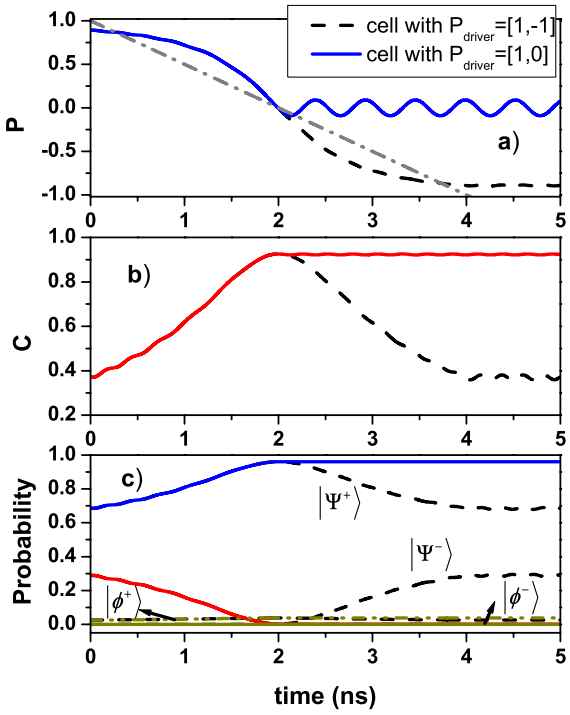

Figure 3. Coherent time evolution of the two DQD cell properties for two changing driver polarization schemes: (i) P_{driver} from $+1$ to -1 (presented with a dash–dot line) in a time $\tau = 4$ ns and (ii) from $+1$ to 0 in time $t_s = \tau/2$. (a) Polarization, (b) concurrence, (c) probabilities for Bell states as a function of time. All cell properties are in dashed and solid lines. We notice that charge densities in the driver cell let us control entangled state formation in the two DQD cell. Parameters: $V = 1$ meV, tunnelling $t/V = 0.03$ and $c = 2a$.

concurrence. Then the concurrence decreases as the contribution of $|\phi^+\rangle$ tends to equal that of $|\Psi^+\rangle$ in the large tunnelling regime.

For coherent dynamics studies (without thermal bath) we evaluate the effect of the driver switching time in the dynamical entanglement formation (we use typical values for $c = 2a$, $t/V = 0.03$ and $\tau = 4$ ns [16]) for the symmetric case with all equal quantum dots ($\delta = 0$).

For a driver polarization changing linearly from $P_{\text{driver}} = +1$ to -1 in a switching time τ, we can observe that the polarization of the two DQD cell (dashed line in figure 3(a)) evolves following that of the driver [16] (dash–dot line in figure 3(a)), changing the two DQD polarization from $P_{\text{cell}} \sim 1$ to ~ -1. Concurrence, on the other hand, increases until it reaches a maximum value at time $t_s \approx \tau/2$ (dashed line in figure 3(b)), and for longer times decreases, reaching an asymptotic value after the driver is completely switched off. We mainly obtain the $|\Psi^+\rangle$ state but there is a small contribution from $|\Psi^-\rangle$, as is shown in the dashed lines in figure 3(c), meaning that the cell is initially very close to the $|01\rangle \sim |\Psi^+\rangle + |\Psi^-\rangle$ state and at τ it completely changes to the state near $|10\rangle| \sim |\Psi^+\rangle - |\Psi^-\rangle$. As we obtain a local maximum of concurrence at $t_s = \tau/2$, we propose to control the system in order to maintain that maximum value by 'turning off' the driver polarization at that time t_s (i.e., P_{driver} goes now from $+1$ to 0 in a time t_s) as presented also in figure 3. We observe stationary properties for polarization, concurrence and Bell state probabilities respectively after the driver depolarizes (solid lines in figures 3(a)–(c)), presenting small oscillations due to coherence. With this dynamical control

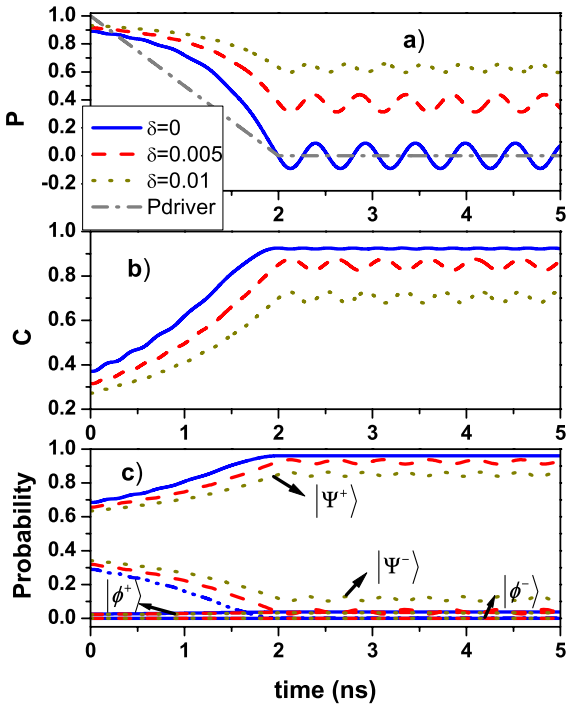

Figure 4. Coherent time evolution of the two DQD cell properties for the entanglement controlled scheme. Driver with polarization P_{driver} from $+1$ to 0 in a time $t_s = \tau/2$ for different asymmetries δ in quantum dot 1. (a) Polarization, (b) concurrence, (c) probabilities for Bell states as a function of time. Notice that asymmetry deteriorates entanglement formation in the two DQD cell (same parameters as in figure 3).

process we are able to generate and maintain one of the Bell states ($|\Psi^+\rangle$) with the largest probability in our system from an almost uncorrelated initial state[3].

In such a *controlled* scheme for entanglement and Bell state $|\Psi^+\rangle$ formation, we include asymmetry effects, $\delta \neq 0$, by decreasing the on-site energy for QD 1 (meaning it has a larger size). The effect of asymmetry on coherent dynamical properties is shown in figure 4. The DQD cell polarization presents a 'delay' with respect to the $\delta = 0$ case even for small values of δ, and almost any change of the polarization is prevented as δ increases [16], as we can see from figure 4(a). Concurrence also presents a delay (figure 4(b)). The system shows a decrease in correlation even for small imperfections, decreasing the concurrence as δ increases. This behaviour is a consequence of cell tendency to trap the electron in site 1; thus the population of states $|10\rangle$ and $|00\rangle$ is inhibited in the dynamics even with the driver effect of equally populating each dot. This effect is also revealed in an increment of the Bell state $|\Psi^-\rangle$ probability and a consequent slight decrease in that of $|\Psi^+\rangle$ (figure 4(c)), meaning that the cell tends to be mainly near the $|01\rangle$ state.

In order to be in the condition of better entanglement formation and evaluate the effect of the phonon environment, we study the case of driver depolarization at time $t_s = \tau/2$ and symmetric dots in the array. In figures 5 and 6 we show results for the dissipative dynamics. We evaluate the effects of temperature in polarization, concurrence and probabilities as a function

[3] The initial condition is chosen as the ground state of the system at the given hopping t/V, for $P_{\text{driver}} = +1$. This yields a smooth behaviour at the start of the driver switching.

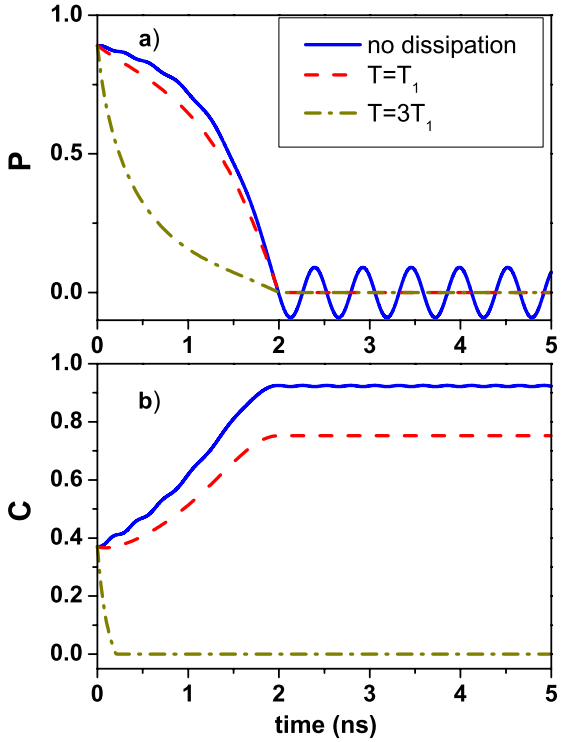

Figure 5. Dissipative dynamics of the two DQD cell for different temperatures. Here $T_1 \sim 1$ K, $D^2 = 0.05$ and we assume symmetric dots. (a) Polarization, (b) concurrence as a function of time (same parameters as in figure 3).

of time. We can observe in figure 5(a) that the cell polarization decreases as the temperature increases, and for high temperature ($T = 3T_1 \approx 3$ K) it is quenched and even seems to ignore the driver effect, in agreement with [16]; the asymptotic polarization value for each temperature is the same (tends to 0) because of the 'turning off' of the driver. On the other hand, concurrence (figure 5(b)) also decreases as the temperature increases. Notice that we obtain entanglement and specifically the $|\Psi^+\rangle$ state (figure 6(a)) for low temperatures $T \sim 1$ K, but it is possible to completely lose correlation for larger temperatures.

As concurrence decreases, we lose the most probable Bell state because the probability of the others begins to increase (figures 6(a)–(d)) due to the bath equilibration process, producing a mixed state with concurrence approaching zero. Notice that oscillations presented in the polarization after driver depolarization are smaller and even disappear because of damping produced by the coupling to the thermal bath. In addition to temperature effects, we observe that dot asymmetry causes the cell to almost completely ignore the driver, yielding a faster decrease in concurrence (results not shown).

Finally, in figure 7 we present the asymptotic stationary behaviour (for times much longer than t_s) of concurrence as a function of temperature. We obtain an entangled state with large concurrence for very low temperature $T < T_1 \approx 1$ K, but there is a fast decay as the temperature increases in the range $T_1 < T < T_c$ due to dissipation effects. We find a critical temperature for our typical parameters of $T_C = T/T_1 \sim 2.4$, where the two DQD cell loses any capability to generate entanglement ($C = 0$); this temperature can depend on the parameters of the DQD cell such as tunnelling and imperfections. This behaviour is better understood if we realize

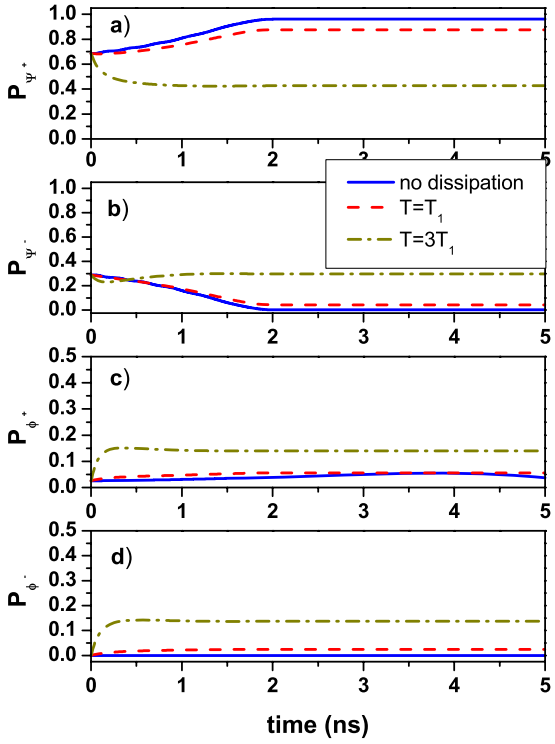

Figure 6. Bell state probabilities obtained in the dissipative dynamics of the two DQD array, for different temperatures ($T_1 \sim 1$ K, $D^2 = 0.05$ and symmetric quantum dots).

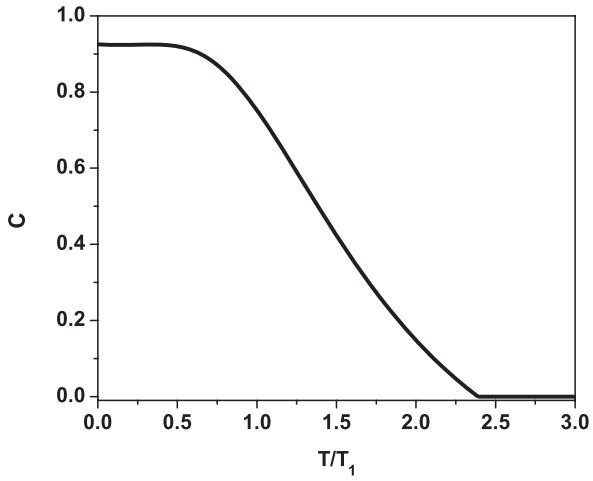

Figure 7. Asymptotic behaviour (long times) of concurrence as a function of temperature for dissipative case and symmetric cell.

that, for long times, the population in each QD tends to be equal because of the equilibration process with the dissipative bath, producing a separable state with the concurrence tending to zero. In such case, the density matrix is diagonal and the eigenvalues of $\rho_S\tilde{\rho}_S$ are equal, so by

definition (equation (9)), the concurrence is zero, meaning that entanglement does not extend to the infinite temperature limit in agreement with treatment presented in [24].

In summary, we have studied the behaviour of polarization, concurrence and Bell state probabilities based on the charge distribution of two mobile electrons in a square array of two double coupled quantum dots. The quantum dynamical evolution of those properties in response to a driver cell whose polarization changes linearly with time, shows a strong dependence on the driver charge distribution, dot imperfections and temperature. Our results show that we can *obtain* and *control* entangled states as well as a most probable $|\Psi^+\rangle$ Bell state via the manipulation of the electrostatic interaction between the two DQD cell and the driver cell. The optimal concurrence and probabilities values calculated can be maintained for low bath temperatures, but are adversely affected by increasing values of temperature and dot imperfection.

Clearly, our results show that it may not be possible to scale this system up to high temperatures and/or to large number of devices; even so, the present theoretical electrostatic mechanism for entanglement formation may be interesting for future experimental conditions where the ability of manipulation of such entangled states could be feasible. Notice that for very low temperatures (from $T \sim 1$ K to $T < 3$ K) the probability for the $|\psi^+\rangle$ state is greater than 0.5, the purification threshold. This opens the theoretical possibility of using some entanglement purification protocols [25] in order to manage mixed states induced by decoherence effects and to produce a pure Bell state. The possible implementation of the two main protocols proposed (IBM [26] and Oxford protocols [27] as well as improved versions of them [28]) requires the use of at least another pair of double quantum dots (that is, a four qubit configuration). The purification is based on the controlled manipulation of single qubit rotations in each pair, classical communication and creation of four qubit correlation by means of the manipulation of two qubits (each one belonging to different pairs), which is the most difficult part of the protocol implementation [25]. This is an interesting problem that can be studied in a future theoretical work. However, for higher temperatures the probability is less than 0.5 and then we will not be able to use entanglement purification.

Furthermore, for the low-temperature regime, this quantum dot array could be used for testing its applicability on a few quantum computation or quantum communication processes where it should not be unreasonable to operate, in a controlled manner, at such temperatures and with the degree of entanglement obtained.

Acknowledgments

This work was supported in part by DGAPA project IN114403 and by CONACyT project 43673-F.

References

[1] Brooks M 1999 *Quantum Computing and Communications* (Cambridge: Springer)
Nielsen M A and Chuang I L 2000 *Quantum Computation and Quantum Information* (Cambridge: Cambridge University Press)
[2] Zeilinger A 1998 *Phys. Scr.* T **76** 203
[3] Riebe M *et al* 2004 *Nature* **429** 734
Barret M B *et al* 2004 *Nature* **429** 737
[4] Weiss S, Thorwart M and Egger R 2006 *Preprint* cond-mat/0601699
[5] Cole T and Lusth J C 2001 *Prog. Quantum Electron.* **25** 165
Hichri A, Jaziri S and Bennaceur R 2004 *Physica* E **24** 234
[6] Itakura T and Tokura Y 2003 *Phys. Rev.* B **67** 195320

[7] Weichselbaum A and Ulloa S E 2004 *Phys. Rev.* A **70** 032328
[8] Pashkin Yu A, Yamamoto T, Astafiev O, Nakamura Y, Averin D V and Tsai J S 2003 *Nature* **421** 823
[9] Liang X T 2005 *Phys. Rev.* B **72** 245328
[10] Fujisawa T, Hayashi T and Hirayama Y 2004 *J. Vac. Sci. Technol.* B **22** 2035
van der Wiel W G, De Francescchi S, Elzerman J M, Fujisawa T, Tarucha S and Kouwenhoven L P 2003 *Rev. Mod. Phys.* **75** 1
[11] Petta J R, Johnson A C, Marcus C M, Hanson M P and Gossard A C 2004 *Phys. Rev. Lett.* **93** 186802
Gorman J, Hasko D G and Williams D A 2005 *Phys. Rev. Lett.* **95** 090502
[12] Tóth G and Lent C S 2001 *Phys. Rev.* A **63** 52315
[13] Lent C S, Tougaw P D and Porod W 1992 *Appl. Phys. Lett.* **62** 714
[14] Amlani I, Orlov A O, Snider G L, Lent C S and Bernstein G H 1998 *Appl. Phys. Lett.* **72** 2179
Amlani I, Orlov A O, Toth G, Bernstein G H, Lent C S and Snider G L 1999 *Science* **284** 289
[15] Gardelis S, Smith C G, Cooper J, Ritchie D A, Linfield E H and Jin Y 2003 *Phys. Rev.* B **67** 33302
[16] Rojas F, Cota E and Ulloa S E 2002 *Phys. Rev.* B **66** 235305
Rojas F, Cota E and Ulloa S E 2000 *Physica* E **6** 428
[17] Lambert N, Aguado R and Brandes T 2006 *Preprint* cond-mat/0602063
[18] Osterloh A, Amico L, Falci G and Fazio R 2002 *Nature* **416** 608
[19] Ausoudeh M and Karimipour V 2005 *Phys. Rev.* A **71** 022308
[20] Wootters W K 1998 *Phys. Rev. Lett.* **80** 2245
[21] Tougaw P D and Lent C S 1996 *J. Appl. Phys.* **80** 4722
[22] Cota E, Rojas F and Ulloa S E 2002 *Phys. Status Solidi* b **230** 377
[23] Mahler G V and Weberruß V A 1995 *Quantum Networks: Dynamics of Open Nanostructures* (Berlin: Springer)
[24] Fine B V, Mintert F and Buchleitner A 2005 *Phys. Rev.* B **71** 153105
[25] Briegel H J 2000 *The Physics of Quantum Information* ed D Bouwmester, A Ekert and A Zeilinger (Berlin: Springer)
[26] Bennett C H, Brassard G, Popescu S, Schumacher B, Smolin J A and Wootters W K 1996 *Phys. Rev. Lett.* **76** 722
Bennett C H, DiVincenzo D P, Smolin J A and Wootters W K 1996 *Phys. Rev.* A **54** 3824
[27] Deutch D, Ekert A, Jozsa R, Macchiavello C, Popescu S and Sanpera A 1996 *Phys. Rev. Lett.* **77** 2818
[28] Metwally N 2002 *Phys. Rev.* A **66** 054302